Single-atom Pd catalyst anchored on Zr-based metal-organic polyhedra for Suzuki-Miyaura cross coupling reactions in aqueous media

Seongsoo Kim[1,§], Seohyeon Jee[2,§], Kyung Min Choi[2] (✉), and Dong-Sik Shin[2] (✉)

[1] Division of Chemical and Bioengineering, Kangwon National University, Gangwon-do 24341, Republic of Korea
[2] Department of Chemical and Biological Engineering, Sookmyung Women's University, 100 Cheongpa-ro 47-gil, Yongsan-gu, Seoul 04310, Republic of Korea
§ Seongsoo Kim and Seohyeon Jee contributed equally to this work.

ABSTRACT

The challenge for single-atom catalysts in various C–C cross coupling reaction exists in the development of solid supporting materials. It has been desired to find a supporting material designed in molecular level to anchor a single-atom catalyst and provide high degree of dispersion and substrate access in aqueous media. Here, we prepared discrete cages of metal-organic polyhedra anchoring single Pd atom (MOP-BPY(Pd)) and successfully performed a Suzuki-Miyaura cross coupling reaction with various substrates in aqueous media. It was revealed that each tetrahedral cage of MOP-BPY(Pd) has 4.5 Pd atoms on average and retained its high degree of dispersion up to 3 months in water. The coupling efficiencies of the Suzuki-Miyaura cross coupling reaction exhibited more than 90.0% for various substrates we have tested in the aqueous media, which is superior to those of the molecular Pd complex and metal-organic framework (MOF) anchoring Pd atoms. Moreover, MOP-BPY(Pd) was successfully recovered and recycled without performance degradation.

KEYWORDS

metal-organic polyhedra, Suzuki-Miyaura cross coupling reaction, structure characterization, aqueous phase reaction, high-degree of dispersion

1   Introduction

The solid supporting materials of heterogeneous catalysts for C–C cross coupling reactions have been developed with the aim of enhancing the atomic efficiency of the active species and carrying out the reactions in aqueous media [1–9]. Particulate supports, such as nanocarbon supports (graphene, graphene oxide) [10–14] and nanoparticles (styrene or silica bead) [15–17], were successful for nanoparticle catalysts, but the challenge has been to anchor the single-atom catalysts in molecular supports to achieve higher catalytic efficiency [18–20]. This is because the molecular supports are mostly successful in amide polar aprotic solvents but lose their activity in aqueous media. Molecular supports have been combined with various solid supporting materials before and after anchoring a single metal species [2] but still have limited use in term of catalyzing the C–C cross-coupling reaction in aqueous media due to agglomeration of the particles, deterioration of the active species, and unpredictable leaching [21–24]. Metal-organic frameworks (MOFs) built by combining molecular supports and inorganic joints have also received attention due to their high periodicity, porosity, and dispersibility [25–28], but the lack of diffusivity for the solvated reactants and products throughout the pores makes it difficult to fully utilize the anchored atomic catalysts. We believe that ultimately small MOFs to the scale of a unit cell would overcome this diffusivity limit and provide vast opportunities as supports for single-atom catalysts in many organic coupling reactions.

Metal-organic polyhedra (MOPs) constructed from organic linkers and inorganic joints have rigid and porous structures similar to those of MOFs, but the interconnecting site in each of the inorganic joint is terminated so that each cell exists independently as a discrete cage (Fig. 1) [29–33]. In particular, a Zr-based MOP is known to be stable in water [34, 35], similar to the Zr-based MOFs of UiO-66 and UiO-67 [36–38], and has a positively charged Zr-oxide cluster to strongly interact with water molecules in aqueous media (Fig. 1) [35, 39]. There are previous reports using pristine MOPs to catalyze various reactions [38, 40–42], but the present work aims to use of MOP as a supporting material for single-atom active species in the catalytic reaction. There are also some cases using MOPs to support single-atom active species for heterogeneous catalysis [43–45] and photocatalysis in organic solvents, but our work prepared chemically stable Zr-based MOPs to support a single-atom catalyst in aqueous media and used them for the C–C coupling reaction.

In this study, we demonstrated that a discrete Zr-based MOP cage anchoring single-atomic PdCl₂ successfully catalyzed Suzuki-Miyaura cross coupling reactions with high activity in aqueous media. Specifically, we prepared a Zr-based MOP using 2,2'-
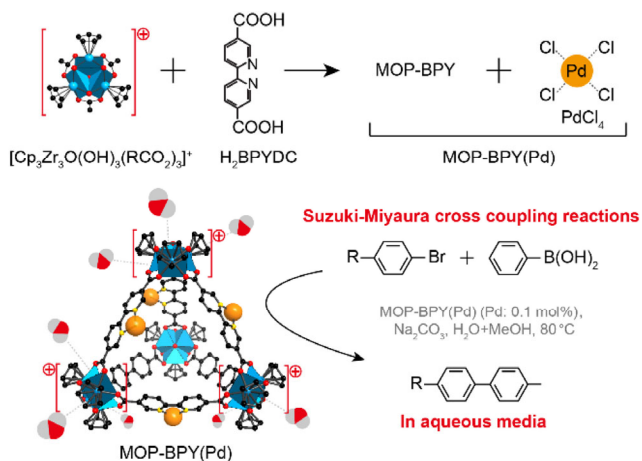

Figure 1 Schematic diagram for the composition and structure of MOP-BPY(Pd) and its application to Suzuki-Miyaura cross coupling reactions in aqueous media.

bipyridine-5,5'-dicarboxylate (BPYDC), hereafter MOP-BPY, and postsynthetically anchored $PdCl_2$ to provide a material referred to herein as MOP-BPY(Pd) (Fig. 1). After characterization of MOP-BPY(Pd) and its dispersion in water, the Suzuki-Miyaura cross coupling efficiencies of MOP-BPY(Pd) were assessed in aqueous media for various bromophenyl derivatives and compared with those for the Pd anchored diester form of BPYDC (hereafter referred to as BPYDE(Pd), (BPYDE = 2,2'-bipyridine-5,5'-diester)) and $PdCl_2$ anchored MOF-867 ($Zr_6O_4(OH)_4$(BPYDC) [38, 39], hereafter referred to as MOF-867(Pd)). MOP-BPY(Pd) exhibits superior coupling efficiencies relative to BPYDE(Pd) and MOF-867(Pd) for derivatives having both an electron-withdrawing and electron-donating group. Moreover, we showed that MOP-BPY(Pd) can be recycled for repeated reactions. The results of this study show that single-atom catalysts can be supported by discrete cages of Zr-based MOPs which have high stability and strong interactions with water, thus expanding the catalysis of C–C cross-coupling reactions in aqueous media.

2 Experimental

2.1 Chemicals

Bis(cyclopentadienyl)zirconium(IV) dichloride (CP_2ZrCl_2), N,N-dimethylformamide (DMF), tetrahydrofuran (THF), triethylamine (TEA), bis(acetonitrile)dichloropalladium(II) ($PdCl_2(CH_2CN)_2$), Na_2CO_3, K_2CO_3, KOH, pyridine, 4-bromoanisole, 4-bromoacetophenone, 4-bromobenzene, phenylboronic acid and acetic acid were purchased from Sigma Aldrich. 4-Bromophenol, 4-bromotoluene, 2-bromothiophene, 4-bromobenzaldehyde, 4-bromoaniline and diethyl ether were purchased from Alfa Aesar. 2,2'-Bipyridine-5,5'-dicarboxylic acid (H_2BPYD), diethyl(2,2'-bipyridine)-5,5'-dicarboxylate and acetonitrile were purchased from TCI. Methanol was purchased from Samchun. All reagents were used as received without further purification.

2.2 Synthesis of MOP-BPY

The MOP-BPY reaction was prepared by dissolving CP_2ZrCl_2 (30 mg, 0.1 mmol) and H_2BPYD (5 mg, 0.03 mmol) in DMF (1 mL) and THF (0.5 mL). Deionized (DI) water (150 μL) was added to the mixture, followed by reaction in an oven at 65 °C for 8 h. After the reaction, white powder was obtained and washed 3 times with DMF (10 mL) using a centrifuge. The MOP crystals were soaked in methanol for 1 day, and then the

MOP cages were obtained via centrifugation and dried *in vacuo*. The synthetic yield of the MOP cage was 86%. The detailed crystallographic and characteristic information was provided in the previous reports [29, 37–39].

2.3 Synthesis of MOP-BPY(Pd)

The as-synthesized MOP-BPY powder (59 mg, 0.05 mmol) and $PdCl_2$ ($CH_2CN)_2$ (14 mg, 0.05 mmol) were dissolved in acetonitrile (2 mL). Followed reaction in an oven at 65 °C for 24 h, the supernatant was decanted by using a centrifuge and washed 3 times with acetonitrile (10 mL) and 3 times with methanol (10 mL). After washing, the solid was obtained via centrifugation and dried *in vacuo*.

2.4 Characterization of materials

The morphology and size of the MOP crystal and MOF were verified by field emission scanning electron microscopy (FE-SEM) with a JEM-7600F, JEOL. The powder sample was dissolved in DMF or methanol and dropped on the holder. Powder X-ray diffraction (PXRD) patterns were obtained by a Bruker D8 Advanced (TRIO/TWIN) at 40 kV and 40 mA. Scanning occurred at a 4 °/min scan rate from 5° to 45° with a silicon holder. Electrospray ionization mass spectroscopy (ESI-MS) was conducted on a triple quadrupole LC-Mass spectrometer (AccuTOF 4G⁺ DART) with samples diluted in methanol. ^1H nuclear magnetic resonance (NMR) data were obtained by a Bruker Advance III HD500. Samples were digested and dissolved by sonication in a mixture of dimethyl sulfoxide-d_6 (DMSO-d_6, 650 μL) and hydrofluoric acid (HF, 150 μL). The digested solution was used directly for ^1H NMR. Fourier transform infrared (FT-IR) spectroscopy was performed on a Thermo Fisher Scientific Nicolet iS50. Sample data were analyzed for ATR diamond mode measurements with 64 scans at a resolution of 4 cm^{-1}. The spectra were recorded in transmission mode. For inductively coupled plasma-optical emission spectroscopy (ICP-OES) analysis, 2.1 mL hydrochloric acid (HCl) and 0.7 mL of nitric acid (HNO_3) were added to 200 μL of MOP-BPY(Pd) aqueous solution (0.5 mg/mL) and digested for 12 h at room temperature (RT). The sample was digested again through Whatman No. 41 filter paper, and 1 mL filtrate was collected in a glass vial for a further dilution (× 10) of 10 mL of aqueous solution. Samples prepared by this method were analyzed by ICP-OES (OPTIMA 7300 DV).

2.5 Suzuki-Miyaura cross coupling reaction

For the Suzuki-Miyaura cross coupling reaction, MOP-BPY(Pd) (0.01 mol% Pd, 100 μg: Pd 0.147 nmol) was dispersed in 1 mL of water and 1 mL of methanol. Then, 4-bromoanisole (27.47 mg, 0.147 mmol) or aryl halides (0.147 mmol), phenylboronic acid (23.28 mg, 191 mmol), and Na_2CO_3, (46.741 mg, 441 mmol) were added to the catalyst solution. For base screening, K_2CO_3, KOH, Na_2CO_3, and pyridine were used under the same conditions. The catalytic reaction was allowed to react at 80 °C for 6–12 h. The corresponding products were obtained by extraction using diethyl ether (2 mL × 3) and were analyzed using gas chromatography (GC, Younglin, YL6100GC).

3 Results and discussion

3.1 Preparation of MOP-BPY(Pd)

Each MOP-BPY has four Zr clusters ($[Cp_3Zr_3O(OH)_3(CO_2)_3]^+$) at the vertices, and each Zr cluster is coordinated to three BPYDC units to form a porous tetrahedral cage (Fig. 1). In the synthesis of MOP-BPY, H_2BPYDC and Cp_2ZrCl_2 were dissolved

together with a mixture of DMF, THF, and DI water, followed by heating at 85 °C for 8 h to give cubic crystals of MOP-BPY. The cubic crystals were formed via the periodic arrangement of MOP-BPY cages. The crystal structure of MOP-BPY was confirmed by PXRD, while the crystal shape was confirmed by FE-SEM. When these crystals were immersed in methanol, the MOP-BPY was unpacked and the resulting species were well dispersed as separated cages. These discrete cages were collected by centrifugation at 8,000 rpm for 10 min and then dried *in vacuo*. To anchor the PdCl$_2$, dried MOP-BPY powder was immersed in acetonitrile containing 0.05 mmol of PdCl$_2$(CH$_2$CN)$_2$ and left in a 65 °C oven for 24 h. The resultant was obtained by centrifugation and dried *in vacuo*. The MOP-BPY and MOP-BPY(Pd) samples were characterized by ESI-MS, ^{1}H NMR spectroscopy, FT-IR spectroscopy, inductively coupled plasma atomic emission spectroscopy (ICP-AES), inductively coupled plasma mass spectroscopy (ICP-MS), and N$_2$ sorption to determine their structures, compositions, molecular configurations and porosities.

3.2 Characterization of MOP-BPY(Pd)

The MOP-BPY crystal was characterized to confirm the structure of MOP-BPY, as it was formed by the periodic arrangement of MOP-BPY cages based on hydrogen bonding between Cl ions and μ$_2$-OH groups in the Zr clusters (Fig. 2(a)). The structure of the MOP-BPY crystal was examined by PXRD. The sharp diffraction patterns indicate a high crystallinity of the crystal, which presents a high-degree of periodic order of MOP-BPY cages in the crystal. The positions of the diffraction lines in 2θ lower than 10° were well matched to those of a model structure having cubic unit cells composed of eight tetrahedral MOP cages packed at each octant position (Fig. 2(b)) [37–39]. The intensities of the diffraction line in 2θ higher than 10° are varied as the inter-distance of the cages highly affected by surroundings of the hydrogen bonding between Cl$^-$ ions and μ$_2$-OH groups in the Zr clusters (Fig. S1 in the Electronic Supplementary Material (ESM)). The shape of the MOP-BPY crystals was cubic

in the reflection of the cubic unit cells (inset of Fig. 2(b)).

Disruption of the hydrogen bonding in the MOP-BPY crystal disassembled and dispersed the MOP-BPY cages well in methanol or water (Fig. 2(c)). After PdCl$_2$ metalation, the mass-to-charge (*m/z*) ratios of the resulting MOP-BPY and MOP-BPY(Pd) cages were determined by ESI-MS (Fig. 2(d)). Prominent peaks for the MOP-BPY cages were observed at *m/z* values of 890.00 and 1,780.00, corresponding to intact [**0**]$^{4+}$ and [**0**]$^{2+}$, respectively (where **0** is a MOP-BPY cage without Cl$^-$ ions). The MOP-BPY(Pd) sample showed *m/z* values of 890.00, 978.3315, 1,022.995, 1,067.326, 1,111.658, 1,155.989, 1,780.00, 1,957.391, 2,045.989, 2,134.652, 2,223.315 and 2,311.978, which are assigned to [**0**]$^{4+}$, [**2**]$^{4+}$, [**3**]$^{4+}$, [**4**]$^{4+}$, [**5**]$^{4+}$, [**6**]$^{4+}$, [**2**]$^{2+}$, [**3**]$^{2+}$, [**4**]$^{2+}$, [**5**]$^{2+}$ and [**6**]$^{2+}$, respectively (where **2**, **3**, **4**, **5** and **6** are the number of PdCl$_2$ in MOP-BPY(Pd) cages). The average number of PdCl$_2$ per cage was determined by the ^{1}H NMR spectrum of MOP-BPY and MOP-BPY(Pd) both digested using HF (Fig. 2(e)). The positions of the NMR peaks indicate the presence of BPYDC and BPYDC(Pd) in the MOP-BPY(Pd) sample. The integration of the peaks confirms that the average number of PdCl$_2$ per cage is 4.5, which corresponds well to the result from ICP-OES elemental analysis. The average number was varied depending on the concentration of the PdCl$_2$ stock solution in metalation process. The number of PdCl$_2$ per cage were 4.425 and 2.4 in the doubled (0.11 M) and half (0.0275 M) concentration of the stock solution, respectively (Fig. S2 in the ESM). Moreover, the average number of PdCl$_2$ was maintained the same after 7 days in methanol, which indicates that there is no spontaneous leaching of Pd from MOP-BPY(Pd). The size of MOP-BPY(Pd) in methanol was measured using dynamic light scattering analysis. The average particle size was about 6 nm (Fig. S3 in the ESM), which indicates that the MOP-BPY(Pd) cages surrounded by solvent molecules exist in discrete form.

The metalation of Pd in MOP-BPY(Pd) was further confirmed by FT-IR spectroscopy (Fig. 2(f)). The absorption at approximately 1,410 and 1,016 cm^{-1}, assigned to C–N and C=N stretching, was significantly decreased after metalation
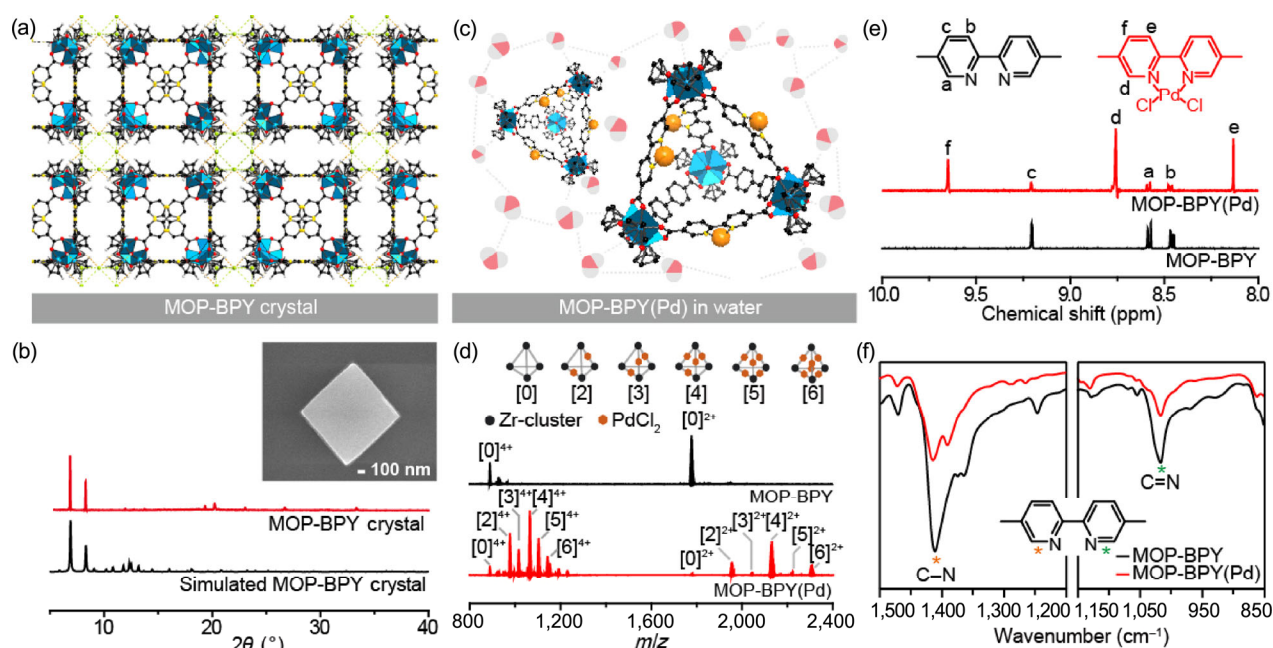

Figure 2 Characterization of MOP-BPY crystal, and MOP-BPY and MOP-BPY(Pd) cages. (a) A schematic of hydrogen bonding between Cl$^-$ ions and μ$_2$-OH groups in a MOP-BPY crystal. (b) PXRD patterns of MOP-BPY crystal compared to its simulated pattern (inset: SEM image of MOP-BPY crystal). (c) A schematic of a MOP-BPY(Pd) cage in water. (d) ESI-MS spectra of MOP-BPY and MOP-BPY(Pd) (6 types of MOP-BPY(Pd) cages with different numbers of Pd; [*X*] = the number of Pd in each cage). (e) Digested ^{1}H NMR spectra of MOP-BPY and MOP-BPY(Pd). (f) FT-IR spectra of MOP-BPY and MOP-BPY(Pd).

compared to the absorption in the MOP-BPY sample. This indicates that PdCl$_2$ is successfully anchored to the sp^2 nitrogen in the BPYDC unit in MOP-BPY(Pd). The porosities of both MOP-BPY and MOP-BPY(Pd) samples were measured by acquiring N$_2$ gas adsorption isotherms (Fig. S4 in the ESM). Compared to the MOP-BPY sample, the MOP-BPY(Pd) sample exhibits a significantly low amount of adsorption indicating that PdCl$_2$ is successfully anchored.

3.3 Degree of dispersion for MOP-BPY(Pd)

The degree of dispersion for MOP-BPY(Pd) was tested in water. Three milligrams of dried MOP-BPY(Pd) was immersed in 20 mL of water and well-dispersed using ultrasonication (Fig. 3(a)). It was speculated that a high degree of dispersion was achieved by the interaction between the positive charge in the metal oxide part of the MOP and the net dipolar nature of the water media. The degree of dispersion of MOP-BPY(Pd) was very high and remained unchanged for three months (Fig. 3). This allows the single-atom Pd catalyst heterogenized on MOP to be well suspended and thus able to catalyze long-lasting catalytic reactions in aqueous media without agglomeration.

3.4 Suzuki-Miyaura cross coupling reaction for MOP-BPY(Pd)

Our initial studies on Suzuki-Miyaura cross coupling focused on the optimization of reaction conditions. We chose 4-bromoanisole and phenylboronic acid as standard substrates and tested their reaction yields in different bases, temperature, reaction time and the amount of MOP-BPY(Pd) (Table 1). For the solvent, methanol was added to water in 1:1 volume ratio to increase the solubility of the substrates. Various bases were tested in the initial reaction condition (described in Table S1 in the ESM), it was found that Na$_2$CO$_3$ showed the higher catalytic activity (78.7%) than K$_2$CO$_3$ (52.2%), KOH (35.4%), and pyridine (1.7%) (Table S1 in the ESM). We speculate that Na$_2$CO$_3$ has suitable cation size, solubility, and pKa than others in this reaction condition [46–48]. The amount of MOP-BPY(Pd) was varied to be 0.1 mol%, 0.05 mol%, and 0.01 mol% to the molar amount of substrates (Table 1, entries 1, 2 and 3). Interestingly, the reaction yield (90.4%) from 0.01 mol% of Pd atom was almost similar to that from 5 and 10 times more Pd amount (90.8% and 91.3% from 0.1 mol% and 0.05 mol% of Pd atom, respectively). The coupling reaction results in higher yield (90.4%) at 80 °C than that (31.3%) at 50 °C, which is due to the activation barrier of overall coupling reaction (Table 1, entries 4 and 5). In the shorter reaction time, the reaction yield was decreased (Table 1, entries 3 and 5).

The catalytic activity of MOP-BPY(Pd) was compared with its molecular (BPYDE(Pd)) and extended form (MOF-867(Pd)). MOF-867 was synthesized from BPYDC and ZrCl$_4$ to give homogeneous size (ca. 100 nm) of particles (Fig. S5 in the ESM). The Pd atom was anchored on MOF-867 in the same procedure

used for MOP-BPY(Pd). The anchoring of Pd atom to the sp^2 nitrogen in BPYDC unit in MOF-867(Pd) was confirmed by IR and NMR spectra (Figs. S6 and S7 in the ESM). The Pd atom was also anchored to the sp^2 nitrogen in BPYDE, which was also confirmed by IR and NMR spectra (Figs. S8 and S9 in the ESM). Then we compared the catalytic yields of MOP-BPY(Pd), BPYDE(Pd), and MOF-867(Pd) for various substrates of 4-bromoacetophenone, 4-bromo aniline, 4-bromobenzaldehyde, 4-bromophenol, 2-bromothiophene, 4-bromoanisole, 12 h (Table 2).

The degree of electron donating and withdrawing effect for substitution groups of the substrates was quantified by ΔV_C calculated from the difference between molecular electrostatic potential at the nucleus of para carbon of the Br-substituted benzene and that of benzene. The larger positive ΔV_C value indicates the higher electron withdrawing effect while the larger negative ΔV_C value shows the higher electron donating effect. The values of ΔV_C are referred from the previous literature [49]. To enhance solubility of hydrophobic substrates (4-bromobenzene and 4-bromotoluene), 10 vol.% of DMF was added. In case of MOP-BPY(Pd), most of aryl bromides were converted to coupling products, regardless of the ΔV_C value of the substrates (Table 2). Although the aryl bromides having electron-withdrawing effect ($\Delta V_C > 0$) usually induce the rate-limiting oxidative addition step [50], it is noteworthy to emphasize that the MOP-BYP(Pd) exhibited more than 90.0% yields for most substrates in aqueous media. Moreover, an electron-rich 4-bromoanisole ($\Delta V_C = -5.0$) also showed high yield (91.2%) (Table 2, entry 6). Among substrates having negative ΔV_C, hydrophobic 4-bromotoluene only yields in moderate (86.2%) (Table 2, entry 5). Even though it is known that the hydrolysis of arylboronic acids disturbs the coupling reaction [51], MOP-BPY(Pd) exhibited superior catalytic yields more than 90.0%. Additionally, the turn-over frequency (TOF) values of MOP-BPY(Pd), BPYDE(Pd), and MOF-BPY(Pd) were summarized in Table S2 in the ESM, indicating that MOP-BPY(Pd) shows superior TOF for all substrates. Consequently, these results indicate that MOP-BPY(Pd) catalyses various substrates in aqueous media.

In case of BPYDE(Pd), most substrates were undesirably coupled with phenylboronic acids, thus the reaction yields were lower than MOP-BPY(Pd) (Table 2, entries 2, 3, 5, 7 and 8). Only oxygen-containing derivatives (1, 4, 6) yielded nearly 90.0%, which could be involved in molecular recognition with the diester groups on ligand and phenylboronic acids via hydrogen bonding interaction [52]. In case of MOF-867(Pd), the catalytic activities were lower than MOP-BPY(Pd) for all substrates (Table 2, entries 1–8). We speculate that this is associated with steric hindrance of solvated substrates and reagents throughout pores arranged from the surface to the core of MOF [53]. Meanwhile, the electron deficient substrates were catalysed well with MOF-867(Pd) (Table 2, entries 1, 3 and 5).
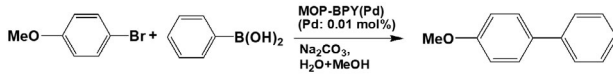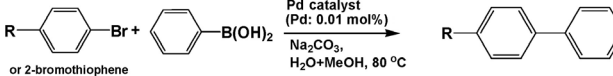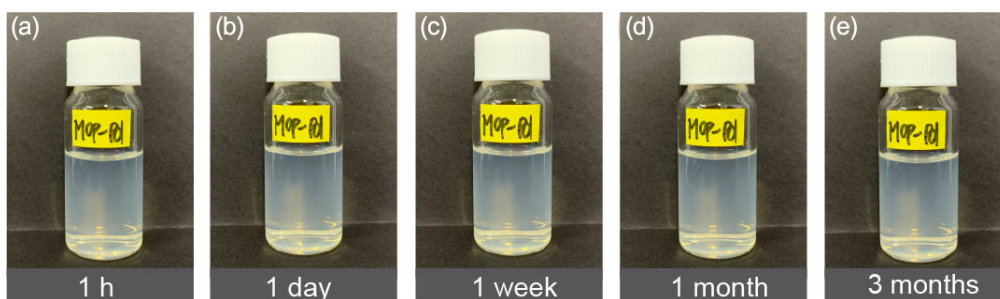

Figure 3 Photos showing the degree of dispersity for MOP-BPY(Pd) in water for 3 months.

Table 1 Suzuki-Miyaura cross coupling reactions for various conditions catalyzed by MOP-BPY(Pd)[a]

MeO—⟨⟩—Br + ⟨⟩—B(OH)₂ →(MOP-BPY(Pd) (Pd: 0.01 mol%), Na₂CO₃, H₂O+MeOH)→ MeO—⟨⟩—⟨⟩

Entry	mol% (Pd)	Time	Temp. (°C)	Yield (%)[b]
1	0.1	12 h	80	91.3
2	0.05	12 h	80	90.8
3	0.01	12 h	80	90.4
4	0.01	4 h	80	78.7
5	0.01	4 h	50	31.3

[a]Conditions: 4-bromoanisole (147 μmol), phenylboronic acid (191 μmol), Na₂CO₃ (441 μmol), 1 mL of MeOH + 1 mL of H₂O, various temperatures (°C), MOP-BPY(Pd) (0.01 mol%–0.1 mol%). [b]GC yield.

Table 2 Coupling efficiencies of various bromophenyl derivatives catalyzed by MOP-BPY(Pd), BPYDE(Pd) and MOF-867(Pd) for the Suzuki-Miyaura cross coupling reactions[a]

R—⟨⟩—Br + ⟨⟩—B(OH)₂ →(Pd catalyst (Pd: 0.01 mol%), Na₂CO₃, H₂O+MeOH, 80 °C)→ R—⟨⟩—⟨⟩
or 2-bromothiophene

Entry: R (or heterocycle)	ΔV_C[b]	Catalyst		
		MOP-BPY (Pd)[c]	BPYDE (Pd)[c]	MOF-867 (Pd)[c]
1. 4-CHO	13.8	94.6	82.9	91.1
2. 4-COCH₃	9.7	98.6	93.8	95.8
3. H	0.0	95.0[d]	83.8[d]	77.6[d]
4. 4-OH	−2.0	93.1	93.0	74.6
5. 4-CH₃	−3.3	86.2[d]	41.6[d]	65.8[d]
6. 4-OCH₃	−5.0	91.2	89.6	75.0
7. 4-NH₂	−9.0	90.1	53.3	78.2
8. 2-Bromothiophene	—	95.7	75.0	90.4

[a]Conditions: 4-bromoanisole (147 μmol), phenylboronic acid (191 μmol), Na₂CO₃ (441 μmol), 1 mL of MeOH + 1 mL of H₂O, 80 °C, catalyst (0.01 mol%). [b]Calculated by Hammett parameter when it is substituted at a hydrogen in benzene [49]. ΔV_C of bromothiophene is not found. [c]GC yields. [d]GC yield by solvent system of 0.8 mL of MeOH + 1.0 mL of H₂O + 0.2 mL of DMF with other conditions the same as in [a].

3.5 Recyclability of MOP-BPY(Pd)

The high stability of Zr-based MOP inspired us to test recyclability of the MOP-BPY(Pd) catalyst in the Suzuki-Miyaura cross coupling reaction. The recovery and re-dispersion of MOP-BPY(Pd) was tested (Figs. 4(a) and 4(b)). The MOP-BPY(Pd) initially dispersed in water was separated well using centrifuge (8,000 rpm) for 10 min (Fig. 4(a)) and re-dispersed again using sonication for 10 min (Fig. 4(b)). Using these behaviours, the recycle yields of MOP-BPY(Pd) was tested using coupling reaction between 4-bromoacetophenone and phenylboronic acid in the presence of Na₂CO₃. After the completion of reaction, the resultant was washed with diethyl ether and water followed by recovering MOP-BPY(Pd) for next reaction. The recycle test was repeated three times. The initial reaction yield (98.6%) remained similar in second (98.6%) and third cycles (98.2%) (Fig. 4(c)). To assess the amount of Pd leached out of MOP-BPY(Pd) after each reaction, the Pd contents were measured by ICP-MS after removing the MOP-BPY(Pd) catalysts. The Pd contents after the 1st, 2nd and 3rd reactions were 114, 59, and 64 μmol/mL of the supernatant solution, which corresponds to 9.0%, 4.6%, and 5.0% of the Pd content (1,260 μmol/mL) existing on MOP-BPY(Pd) before the reaction, respectively (Fig. S11 in the ESM). These results indicate that there is partial leaching of Pd during the catalytic reaction but it is not significant considering the reaction yield remained almost the same after the 3rd reaction
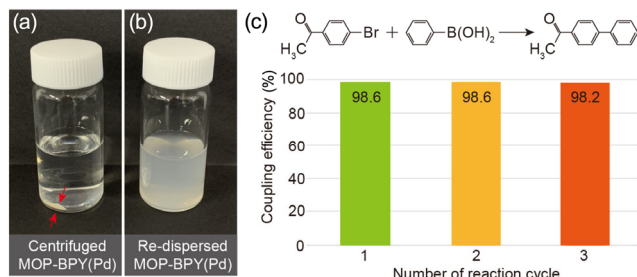
Figure 4 Reusability test of MOP-BPY(Pd). Snapshots of MOP-BPY(Pd) solution (a) after centrifuge and (b) re-dispersion. (c) Recyclability of MOP-BPY(Pd) for the Suzuki-Miyaura cross coupling reaction of 4-bromoacetophenone with phenylboronic acid.

cycles (Fig. 4(c)). We also ran the reaction using the supernatant after 1st reaction cycle, and found that there was no activity. We envision that Zr-based MOP-BPY can support various single-atom catalysts, thus catalyze other C–C coupling reactions with high activity, stability, and recyclability in aqueous media.

4 Conclusion

We have explored a MOP-BPY supporting single Pd atom as a new heterogeneous catalyst for the Suzuki-Miyaura cross coupling reaction. The structure and physicochemical features of MOP-BPY(Pd) was characterized, and the existence of 4.5 Pd atoms on each MOP cage was also revealed. Suzuki-Miyaura cross coupling reactions were performed with MOP-BPY(Pd) in aqueous solution. The catalytic activity of MOP-BPY(Pd) with various substrates were superior to those of BPYDE(Pd) and MOF-867(Pd). Overall the advantage of this catalytic reaction is due to the structure of MOP designed to anchor a Pd atomic catalyst as well as the discreteness of MOP cages well dispersed in the aqueous media. We envision that MOP-BPY(Pd) or other derivatives will be used for various catalytic reactions.

Acknowledgements

References

[1] Zhang, L. L.; Wang, A. Q.; Miller, J. T.; Liu, X. Y.; Yang, X. F.; Wang, W. T.; Li, L.; Huang, Y. Q.; Mou, C. Y.; Zhang, T. Efficient and durable Au alloyed Pd single-atom catalyst for the ullmann reaction of aryl chlorides in water. *ACS Catal*. **2014**, *4*, 1546–1553.

[2] Zhang, X. Y.; Sun, Z. C.; Wang, B.; Tang, Y.; Nguyen, L.; Li, Y. T.; Tao, F. F. C–C coupling on single-atom-based heterogeneous catalyst. *J. Am. Chem. Soc*. **2018**, *140*, 954962.

[3] Fernández, E.; Rivero-Crespo, M. A.; Domínguez, I.; Rubio-Marqués, P.; Oliver-Meseguer, J.; Liu, L. C.; Cabrero-Antonino, M.; Gavara, R.; Hernández-Garrido, J. C.; Boronat, M. et al. Base-controlled Heck, Suzuki, and Sonogashira reactions catalyzed by ligand-free platinum or palladium single atom and sub-nanometer clusters. *J. Am. Chem. Soc*. **2019**, *141*, 1928–1940.

[4] Yin, L. X.; Liebscher, J. Carbon-carbon coupling reactions catalyzed by heterogeneous palladium catalysts. *Chem. Rev*. **2007**, *107*, 133–173.

[5] Veerakumar, P.; Thanasekaran, P.; Lu, K. L.; Lin, K. C.; Rajagopal, S. Computational studies of versatile heterogeneous palladium-catalyzed

Suzuki, Heck, and Sonogashira coupling reactions. *ACS Sustain. Chem. Eng.* **2017**, *5*, 8475–8490.

[6] Bernini, R.; Cacchi, S.; Fabrizi, G.; Forte, G.; Petrucci, F.; Prastaro, A.; Niembro, S.; Shafir, A.; Vallribera, A. Perfluoro-tagged, phosphine-free palladium nanoparticles supported on silica gel: Application to alkynylation of aryl halides, Suzuki-Miyaura cross-coupling, and Heck reactions under aerobic conditions. *Green Chem.* **2010**, *12*, 150–158.

[7] Biffis, A.; Zecca, M.; Basato, M. Palladium metal catalysts in Heck C–C coupling reactions. *J. Mol. Catal. A Chem.* **2001**, *173*, 249–274.

[8] Suzaki, Y.; Kobayashi, Y.; Tsuchido, Y.; Osakada, K. Pd-catalyzed Sonogashira coupling in aqueous media. Observation of micelles that contain substrates and catalyst. *Mol. Catal.* **2019**, *466*, 106–111.

[9] Christoffel, F.; Ward, T. R. Palladium-catalyzed heck cross-coupling reactions in water: A comprehensive review. *Catal. Lett.* **2018**, *148*, 489–511.

[10] Lakshminarayana, B.; Mahendar, L.; Ghosal, P.; Satyanarayana, G.; Subrahmanyam, C. Nano-sized recyclable PdO supported carbon nanostructures for Heck reaction: Influence of carbon materials. *ChemistrySelect* **2017**, *2*, 2700–2707.

[11] Tran, T. P. N.; Thakur, A.; Trinh, D. X.; Dao, A. T. N.; Taniike, T. Design of Pd@graphene oxide framework nanocatalyst with improved activity and recyclability in Suzuki-Miyaura cross-coupling reaction. *Appl. Catal. A*: *Gen* **2018**, *549*, 60–67.

[12] Diyarbakir, S.; Can, H. S.; Metin, O. Reduced graphene oxide-supported CuPd alloy nanoparticles as efficient catalysts for the Sonogashira cross-coupling reactions. *ACS Appl. Mater. Interfaces* **2015**, *7*, 3199–3206.

[13] Sharavath, V.; Ghosh, S. Palladium nanoparticles on noncovalently functionalized graphene-based heterogeneous catalyst for the Suzuki-Miyaura and Heck-Mizoroki reactions in water. *RSC Adv.* **2014**, *4*, 48322–48330.

[14] Scheuermann, G. M.; Rumi, L.; Steurer, P.; Bannwarth, W.; Mülhaupt, R. Palladium nanoparticles on graphite oxide and its functionalized graphene derivatives as highly active catalysts for the Suzuki-Miyaura coupling reaction. *J. Am. Chem. Soc.* **2009**, *131*, 8262–8270.

[15] Balaswamy, K.; Pullaiah, P. C.; Srinivas, K.; Rao, M. M. Polystyrene-supported palladium(II) N,N-dimethylethylenediamine complex: A recyclable catalyst for Suzuki-Miyaura cross-coupling reactions in water. *Inorg. Chim. Acta* **2014**, *423*, 95–100.

[16] Moussa, S.; Siamaki, A. R.; Gupton, B. F.; El-Shall, M. S. Pd-partially reduced graphene oxide catalysts (Pd/PRGO): Laser synthesis of Pd nanoparticles supported on PRGO nanosheets for carbon–carbon cross coupling reactions. *ACS Catal.* **2012**, *2*, 145–154.

[17] De Castro, K. A.; Rhee, H. Resin-immobilized palladium nanoparticle catalysts for Suzuki-Miyaura cross-coupling reaction in aqueous media. *J. Incl. Phenom. Macrocycl. Chem.* **2015**, *82*, 13–24.

[18] Chen, L. Y.; Rangan, S.; Li, J.; Jiang, H. F.; Li, Y. W. A molecular Pd(II) complex incorporated into a MOF as a highly active single-site heterogeneous catalyst for C–Cl bond activation. *Green Chem.* **2014**, *16*, 3978–3985.

[19] Nagai, D.; Goto, H. Effective heterogeneous catalyst for Suzuki-Miyaura cross-coupling in aqueous media: Melamine cyanurate complex containing Pd species. *Bull. Chem. Soc. Jpn.* **2018**, *91*, 147–152.

[20] Yang, Y.; Reber, A. C.; Gilliland III, S. E.; Castano, C. E.; Gupton, B. F.; Khanna, S. N. More than just a support: Graphene as a solid-state ligand for palladium-catalyzed cross-coupling reactions. *J. Catal.* **2018**, *360*, 20–26.

[21] Dighe, M. G.; Lonkar, S. L.; Degani, M. S. Mechanistic insights into palladium leaching in novel Pd/C-catalyzed boron-Heck reaction of arylboronic acid. *Synlett* **2013**, *24*, 347–350.

[22] Veerakumar, P.; Thanasekaran, P.; Lu, K. L.; Liu, S. B.; Rajagopal, S. Functionalized silica matrices and palladium: A versatile heterogeneous catalyst for Suzuki, Heck, and Sonogashira reactions. *ACS Sustain. Chem. Eng.* **2017**, *5*, 6357–6376.

[23] MacQuarrie, S.; Horton, J. H.; Barnes, J.; McEleney, K.; Loock, H. P.; Crudden, C. M. Visual observation of redistribution and dissolution of palladium during the Suzuki-Miyaura reaction. *Angew. Chem., Int. Ed.* **2008**, *47*, 3279–3282.

[24] Richardson, J. M.; Jones, C. W. Strong evidence of solution-phase catalysis associated with palladium leaching from immobilized thiols during Heck and Suzuki coupling of aryl iodides, bromides, and chlorides. *J. Catal.* **2007**, *251*, 80–93.

[25] Huang, Y. B.; Zheng, Z. L.; Liu, T. F.; Lü, J.; Lin, Z. J.; Li, H. F.; Cao, R. Palladium nanoparticles supported on amino functionalized metal-organic frameworks as highly active catalysts for the Suzuki-Miyaura cross-coupling reaction. *Catal. Commun.* **2011**, *14*, 27–31.

[26] Kardanpour, R.; Tangestaninejad, S.; Mirkhani, V.; Moghadam, M.; Mohammadpoor-Baltork, I.; Khosropour, A. R.; Zadehahmadi, F. Highly dispersed palladium nanoparticles supported on amino functionalized metal-organic frameworks as an efficient and reusable catalyst for Suzuki cross-coupling reaction. *J. Organomet. Chem.* **2014**, *761*, 127–133.

[27] Puthiaraj, P.; Ahn, W. S. Highly active palladium nanoparticles immobilized on NH₂-MIL-125 as efficient and recyclable catalysts for Suzuki-Miyaura cross coupling reaction. *Catal. Commun.* **2015**, *65*, 91–95.

[28] Fei, H. H.; Cohen, S. M. A robust, catalytic metal-organic framework with open 2,2'-bipyridine sites. *Chem. Commun.* **2014**, *50*, 4810–4812.

[29] Nam, D.; Huh, J.; Lee, J.; Kwak, J. H.; Jeong, H. Y.; Choi, K.; Choe, W. Cross-linking Zr-based metal-organic polyhedra via postsynthetic polymerization. *Chem. Sci.* **2017**, 8, 7765–7771.

[30] Mollick, S.; Fajal, S.;Mukherjee, S.; Ghosh, S. K. Stabilizing metal-organic polyhedra (MOP): Issues and strategies. *Chem.—Asian J.* **2019**, *14*, 3096–3108.

[31] Wang, W.; Wang, Y. X.; Yang, H. B. Supramolecular transformations within discrete coordination-driven supramolecular architectures. *Chem. Soc. Rev.* **2016**, *45*, 2656–2693.

[32] Li, J. R.; Zhou, H. C. Bridging-ligand-substitution strategy for the preparation of metal-organic polyhedra. *Nat. Chem.* **2010**, *2*, 893–898.

[33] Tranchemontagne, D. J.; Ni, Z.; O'Keeffe, M.; Yaghi, O. M. Reticular chemistry of metal-organic polyhedra. *Angew. Chem., Int. Ed.* **2008**, *47*, 5136–5147.

[34] Lu, Z.; Knobler, C. B.; Furukawa, H.; Wang, B.; Liu, G. N.; Yaghi, O. M. Synthesis and structure of chemically stable metal-organic polyhedra. *J. Am. Chem. Soc.* **2009**, *131*, 12532–12533.

[35] Xing, W. H.; Li, H. Y.; Dong, X. Y.; Zang, S. Q. Robust multifunctional Zr-based metal-organic polyhedra for high proton conductivity and selective CO₂ capture. *J. Mater. Chem. A* **2018**, *6*, 7724–7730.

[36] Ju, Z. F.; Liu, G. L.; Chen, Y. S.; Yuan, D. Q.; Chen, B. L. From coordination cages to a stable crystalline porous hydrogen-bonded framework. *Chem.—Eur. J.* **2017**, *23*, 4774–4777.

[37] Liu, G. L.; Ju, Z. F.; Yuan, D. Q.; Hong, M. C. *In situ* construction of a coordination zirconocene tetrahedron. *Inorg. Chem.* **2013**, *52*, 13815–13817.

[38] Liu, G. L.; Zeller, M.; Su, K. Z.; Pang, J. D.; Ju, Z. F.; Yuan, D. Q.; Hong, M. C. Controlled orthogonal self-assembly of heterometal-decorated coordination cages. *Chem.—Eur. J.* **2016**, *22*, 17345–17350.

[39] Lee, H. S.; Jee, S.; Kim, R.; Bui, H. T.; Kim, B.; Kim, J. K.; Park, K. S.; Choi, W.; Kim W.; Choi, K. M. A highly active, robust photocatalyst heterogenized in discrete cages of metal-organic polyhedra for CO₂ reduction. *Energy Environ. Sci.* **2020**, *13*, 519–526

[40] Choi, K. M.; Jeong, H. M.; Park, J. H.; Zhang, Y. B.; Kang, J. K.; Yaghi, O. M. Supercapacitors of nanocrystalline metal-organic frameworks. *ACS Nano* **2014**, *8*, 7451–7457.

[41] Kang, Y. H.; Liu, X. D.; Yan, N.; Jiang, Y.; Liu, X. Q.; Sun, L. B.; Li, J. R. Fabrication of isolated metal-organic polyhedra in confined cavities: Adsorbents/catalysts with unusual dispersity and activity. *J. Am. Chem. Soc.* **2016**, *138*, 6099–6102.

[42] Lin, W. G.; Yuan, D. Q.; Yakovenko, A.; Zhou, H. C. Surface functionalization of metal–organic polyhedron for homogeneous cyclopropanation catalysis. *Chem. Commun.* **2011**, *47*, 4968–4970.

[43] Vardhan, H.; Verpoort, F. Metal-organic polyhedra: Catalysis and reactive intermediates. *Adv. Synth. Catal.* **2015**, *357*, 1351–1368.

[44] Maity, K.; Karan, C. K.; Biradha, K. Porous metal-organic polyhedral framework containing cuboctahedron cages as SBUs with high affinity for H₂ and CO₂ sorption: A heterogeneous catalyst for chemical fixation of CO₂. *Chem.—Eur. J.* **2018**, *24*, 10988–10993.

[45] Ahmad, N.; Younus, H. A.; Chughtai, A. H.; Van Hecke, K.; Danish, M.; Gaoke, Z.; Verpoort, F. Development of mixed metal metal-organic polyhedra networks, colloids, and MOFs and their pharmacokinetic applications. *Sci. Rep.* **2017**, *7*, 832.

[46] Sherwood, J.; Clark, J. H.; Fairlamb, I. J. S.; Slattery, J. M. Solvent effects in palladium catalysed cross-coupling reactions. *Green Chem.* **2019**, *21*, 2164–2213.

[47] Lima, C. F. R. A. C.; Rodrigues, A. S. M. C.; Silva, V. L. M.; Silva, A. M. S.; Santos, L. M. N. B. F. Role of the base and control of selectivity in the Suzuki-Miyaura cross-coupling reaction. *ChemCatChem.* **2014**, *6*, 1291–1302.

[48] Zhang, H. C.; Kwong, F. Y.; Tian, Y.; Chan, K. S. Base and cation effects on the Suzuki cross-coupling of bulky arylboronic acid with halopyridines: Synthesis of pyridylphenols. *J. Org. Chem.* **1998**, *63*, 6886–6890.

[49] Remya, G. S.; Suresh, C. H. Quantification and classification of substituent effects in organic chemistry: A theoretical molecular electrostatic potential study. *Phys. Chem. Chem. Phys.* **2016**, *18*, 20615–20626.

[50] Littke, A. F.; Dai, C. Y.; Fu, G. C. Versatile catalysts for the Suzuki cross-coupling of arylboronic acids with aryl and vinyl halides and triflates under mild conditions. *J. Am. Chem. Soc.* **2000**, *122*, 4020–4028.

[51] Watanabe, T.; Miyaura, N.; Suzuki, A. Synthesis of sterically hindered biaryls via the palladium-catalyzed cross-coupling reaction of arylboronic acids or their esters with haloarenes. *Synlett* **1992**, *1992*, 207–210.

[52] Fournier, J. H.; Maris, T.; Wuest, J. D.; Guo, W. Z.; Galoppini, E. Molecular tectonics. Use of the hydrogen bonding of boronic acids to direct supramolecular construction. *J. Am. Chem. Soc.* **2003**, *125*, 1002–1006.

[53] Dhakshinamoorthy, A.; Alvaro, M.; Hwang, Y. K.; Seo, Y. K.; Corma, A.; Garcia, H. Intracrystalline diffusion in metal organic framework during heterogeneous catalysis: Influence of particle size on the activity of MIL-100 (Fe) for oxidation reactions. *Dalton Trans.* **2011**, *40*, 10719–10724.